Analysis of the Mechanical Behavior, Microstructure, and Reliability of Mixed Formulation Solder Joints

Yifei Zhang, Kanth Kurumaddali, Jeffrey C. Suhling, Pradeep Lall, Michael J. Bozack
Center for Advanced Vehicle Electronics
Auburn University
Auburn, AL 36849
Phone: +1-334-844-3332
FAX: +1-334-844-3307
E-Mail: jsuhling@eng.auburn.edu

Abstract

The transition from tin-lead to lead free soldering in the electronics manufacturing industry has been in progress for the past 10 years. In the interim period before lead free assemblies are uniformly accepted, mixed formulation solder joints are becoming commonplace in electronic assemblies. For example, area array components (BGA/CSP) are frequently available only with lead free Sn-Ag-Cu (SAC) solder balls. Such parts are often assembled to printed circuit boards using traditional 63Sn-37Pb solder paste. The resulting solder joints contain unusual quaternary alloys of Sn, Ag, Cu, and Pb. In addition, the alloy composition can vary across the solder joint based on the paste to ball solder volumes and the reflow profile utilized. The mechanical and physical properties of such Sn-Ag-Cu-Pb alloys have not been explored extensively in the literature. In addition, the reliability of mixed formulation solder joints is poorly understood.

In this work, we have explored the physical properties and mechanical behavior of mixed formulation solder materials. Seven different mixture ratios of 63Sn-37Pb and SAC305 solder materials have been formed, which include five carefully controlled mixtures of the two solder alloys (by weight percentage) and the two extreme cases (pure Sn-Pb and pure SAC). For the various percentage mixtures, the melting point, pasty range, stress-strain curves, mechanical properties (modulus, strength), and creep curves have been characterized. The variations of the mechanical properties and creep rates with aging at room temperature (25 ^{o}C) and elevated temperature (100 ^{o}C) have also been measured. Finally, the microstructures realized with the various mixtures have been found and correlated to the mechanical measurements and microstructures found in actual mixed formulation BGA solder joints. The results for the mechanical and physical properties show a very complicated dependence on the mixture ratio.

Introduction

Even though many countries have stated deadlines for the completion of the tin-lead to lead free soldering transition, many critical issues have not been resolved due to the incomplete infrastructure for lead free soldering technology, as well as the timing and technical readiness in the various sectors of the electronics manufacturing industry. Therefore, companies often face an interim period of "mixed assembly" where lead free components are used with tin-lead solder paste, or tin-lead plated components or printed circuit boards are used with lead-free solder paste. The presence of so-called "mixed formulation" solder joints or "mixed solders" is often unavoidable due to unavailability of components with the desired finish or careless suppliers providing components that do not meet the specifications of the manufacturer doing the SMT assembly.

There are two kinds of mixed assemblies defined by the conditions that the solder balls, platings, and pastes are combined [1-6]. When the older "standard" Sn-Pb pastes and processes are mixed with components with SAC solder balls or component leads with SAC finishes, the process is referred to as a "backward compatible" process (see Figure 1). Likewise, when SAC pastes and processes are mixed with components with Sn-Pb solder balls or components/PCBs with Sn-Pb surface finishes, the process is referred to as a "forward compatible" process. The metallurgical reaction of Sn-Ag-Cu and Sn-Pb is a secondary alloying process and two different micro-structural scenarios typically result: (1) fully-mixed joint, and (2) partially mixed joint. There is a 34 °C temperature difference between the eutectic temperature of the Sn-Ag-Cu system (217 °C) and the eutectic temperature of the Sn-Pb system (183 °C). The homogeneity of a mixed Pb and Sn-Ag-Cu structure is driven by Pb diffusion in the solder joint and determined by such factors as Pb concentration, peak reflow temperature and dwell time, soldering environment, and lead-free solder composition [7]. For example, SEM microstructures of cross-sectioned mixed formulation BGA solder joints that are well mixed and poorly mixed are shown in Figures 2 and 3, respectively. In these cases, the degree of mixing was controlled by adjusting the peak reflow temperature and the dwell at the peak temperature. Further examples of poor mixing can be found in the literature [8-10].

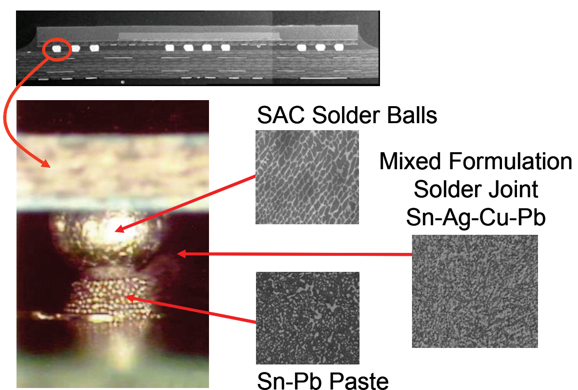

Figure 1 - Mixed Assembly (Backward Compatibility)

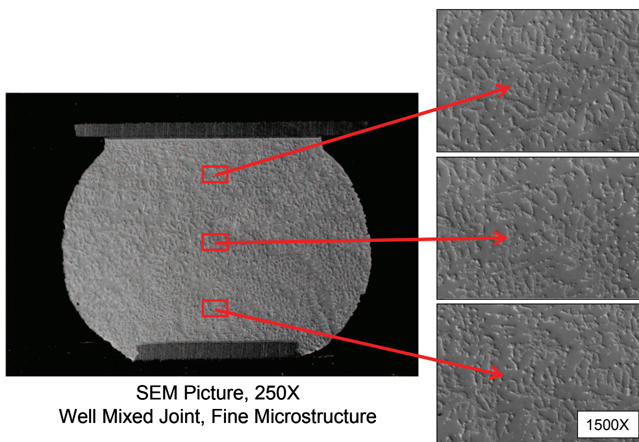

Figure 2 - SEM Micrograph of Well-Mixed BGA Joint

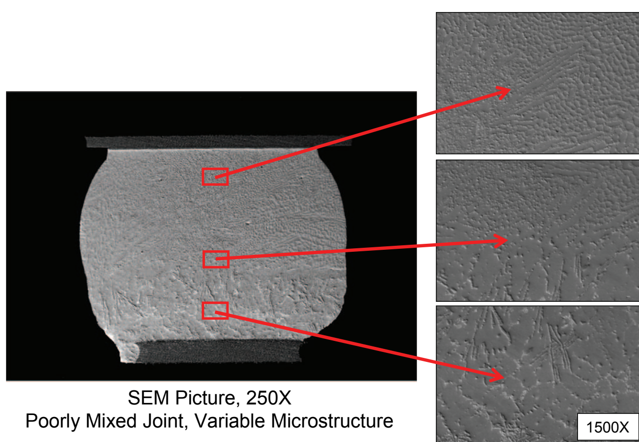

Figure 3 - SEM Micrograph of Poorly Mixed BGA Joint

Maintaining solder joint reliability is the key challenge in the transition to lead free, and questions always occur when the mixing of tin-lead and lead free materials and processes occur. Contradictory research results regarding mixed soldering have been found in the literature [8]. Some studies have showed enhanced mechanical properties and reliabilities in solder joints formed by mixing Sn-Ag-Cu and Pb, whereas other studies reported deteriorated performance. Two topics that are often debated include: (1) the minimum peak temperature and dwell time above liquidous (TAL) required for reliable backward assembly, and (2) the best methods to achieve optimal homogeneity and reliability of mixed solder joints. High peak temperatures are usually used in reflowing lead-free solder joints due to the high SAC melting temperature in order to obtain a homogenous microstructure. However, high reflow temperatures will often cause assembly challenges and reliability concerns.

Hua, et al. [4, 11] have concluded that reliability and process risks are high for backward solder joints formed with a reflow profile with peak temperature less than 217 °C. Low temperatures resulted in inhomogeneous microstructures and partially collapsed Sn-Ag-Cu solder balls. The same phenomenon was also observed by Zbrzezny, et al. [9]. Theuss and coworkers [12] further stated that a peak temperature of at least 235 ºC is needed to obtain acceptable reliability of backward compatible solder joints. On the contrary, Nandagopal, et al. [1, 13] found that backward solder joints with fully mixed microstructure could be achieved with a peak reflow temperature of about 210°C and within 20-30 second dwell times for certain paste to ball weight ratios. Nguyen, et al. [14] found that complete mixing of SnPb solder with SnAgCu depends on the volume of the SnPb solder paste relative to that of the SnAgCu ball, and the soldering temperature. They concluded that proper mixing can result for reflow temperatures below 217 ºC if the right amount of SnPb solder paste is used. Finally, Sun and coworkers [15] reported good reliability and relatively homogenous microstructure with reflow peak temperatures between 183-220 ºC.

Several other investigations on backward compatibility processes have been undertaken including: (1) evaluating Pb diffusion and the phases formed in solder mixtures containing Sn-Pb and Sn-Ag-Cu alloys [16-17]; (2) evaluation of the reliability of mixed solder joints for various components under different accelerated thermal cycling environments [2, 5-6, 18-19]; (3) measurement of the properties and failure modes of mixed solder joints under mechanical and shock loadings [18, 20-21]; and (4) use of finite element analysis to predict mixed solder joint reliability [22].

In this work, we have explored the physical properties and mechanical behavior of mixed formulation solder materials. Seven different mixture ratios of 63Sn-37Pb and SAC305 solder materials have been formed, which include five carefully controlled mixtures of the two solder alloys (by weight percentage) and the two extreme cases (pure Sn-Pb and pure SAC). For the various percentage mixtures, the melting point, pasty range, stress-strain curves, mechanical properties (modulus, strength, elongation), and creep curves have been characterized. The variations of the mechanical properties and creep rates with aging at room temperature (25 ^{o}C) and elevated temperature (100 ^{o}C) have also been measured. Finally, the microstructures realized with the various mixtures have been found and correlated to the mechanical measurements and microstructures found in actual mixed formulation BGA solder joints.

Experimental Method

Preparation of Mixed Formulation Solders

Solders with seven different mixture ratios of 63Sn-37Pb and SAC305 solder materials have been formed. Two of these were the pure solder alloys (63Sn-37Pb and SAC305), and five were mixtures controlled by the weight percentages of the two alloys. In this work, we refer to each mixed alloy with the nomenclature MIX A-B, where A and B are the weight percentages of 63Sn-37Pb and SAC305, respectively, in the mixture. For example, MIX 30-70 is a solder mixture of 30 wt% 63Sn-37Pb and 70 wt% SAC305. The chemical compositions of the seven solder alloys are listed in Figure 4.

Uniaxial Test Sample Preparation

Solder samples for mechanical characterization were prepared using a novel procedure where molten solder was

drawn into high precision rectangular cross-section glass tubes using a vacuum suction process. The solder is first melted in a quartz crucible using a pair of circular heating elements (see Figure 5). A thermocouple attached on the crucible and a temperature control module is used to direct the melting process. One end of the glass tube is inserted into the molten solder, and suction is applied to the other end via a rubber tube connected to the house vacuum system. The suction forces are controlled through a regulator on the vacuum line so that only a desired amount of solder is drawn into the tube. The tubes were then cooled by water quenching (Figure 6) to yield a fine microstructure, and the upper limits of the mechanical properties and the lower limits of the possible creep rates.

Solder Type	%Sn	%Pb	%Ag	%Cu
MIX 0-100 (SAC305)	96.50	0	3.00	0.50
MIX 10-90	93.15	3.70	2.70	0.45
MIX 30-70	86.45	11.10	2.10	0.35
MIX 50-50	79.75	18.50	1.50	0.25
MIX 70-30	73.05	25.90	0.90	0.15
MIX 90-10	66.35	33.30	0.30	0.05
MIX 100-0 (63Sn-37Pb)	63.00	37.00	0	0

Figure 4 - Table of Mixed Solder Alloys

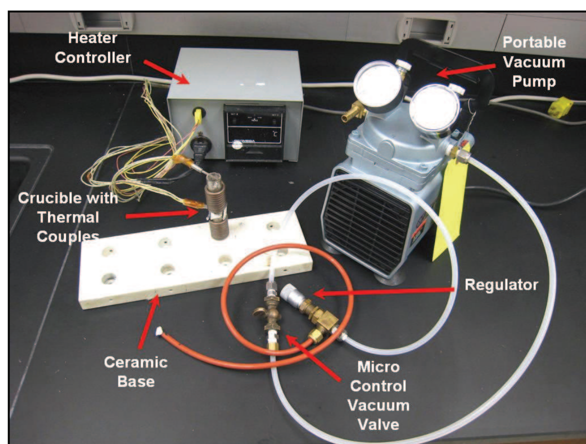

Figure 5 - Specimen Preparation Hardware

Typical glass tube assemblies filled with solder and a final extracted specimen are shown in Figure 7. The final test specimen dimensions are governed by the useable length of the tube that can be filled with solder, and the cross-sectional dimensions of the hole running the length of the tube. In the current work, we formed uniaxial samples with nominal dimensions of 80 x 3 x 0.5 mm. A thickness of 0.5 mm was chosen because it matches the height of typical BGA solder balls. After solidification and cooling, samples were aged at 25 ^{o}C (room temperature) or 100 ^{o}C for various periods before mechanical testing.

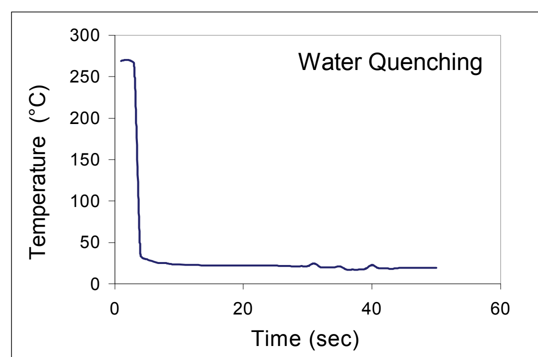

Figure 6 - Cooling Profile

(a) Within Glass Tubes

(b) After Extraction

Figure 7 - Solder Uniaxial Test Specimens

The described sample preparation procedure yielded repeatable samples with controlled cooling profile (i.e. microstructure), oxide free surface, and uniform dimensions. By extensively cross-sectioning several specimens, we have verified that the microstructure of any given sample is consistent throughout the volume of the sample. In addition, we have established that our method of specimen preparation yields repeatable sample microstructures for a given solidification temperature profile. Samples were inspected using a micro-focus x-ray system to detect flaws (e.g. notches and external indentations) and/or internal voids (non-visible). With proper experimental techniques, samples with no flaws and voids were generated.

Mechanical Testing System

A MT-200 tension/torsion thermo-mechanical test system from Wisdom Technology, Inc., as shown in Figure 8, has been used to test the samples in this study. The system provides an axial displacement resolution of 0.1 micron and a rotation resolution of 0.001°. Testing can be performed in tension, shear, torsion, bending, and in combinations of these loadings, on small specimens such as thin films, solder joints, gold wire, fibers, etc. Cyclic (fatigue) testing can also be performed at frequencies up to 5 Hz. In addition, a universal 6-axis load cell was utilized to simultaneously monitor three

forces and three moments/torques during sample mounting and testing. Environmental chambers added to the system allow samples to be tested over a temperature range of -185 to +300 °C.

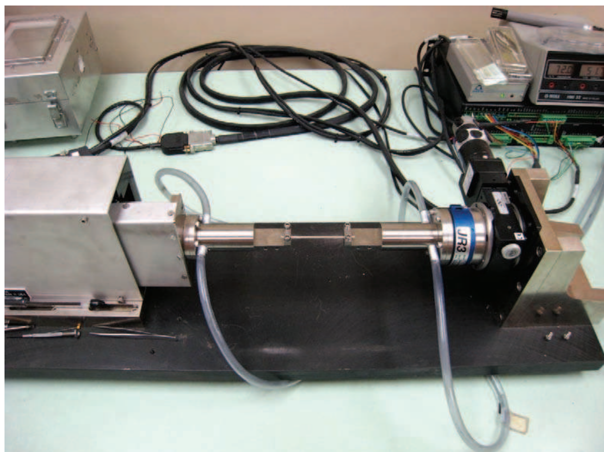

Figure 8 - MT-200 Testing System with Solder Sample

During uniaxial testing, forces and displacements were measured. The axial stress and axial strain were calculated from the applied force and measured cross-head displacement using

$$\sigma = \frac{F}{A} \qquad \varepsilon = \frac{\Delta L}{L} = \frac{\delta}{L} \tag{1}$$

where σ is the uniaxial stress, ε is the uniaxial strain, F is the measured uniaxial force, A is the original cross-sectional area, δ is the measured crosshead displacement, and L is the specimen gage length (initial length between the grips). The gage length of the specimens in this study was 60 mm, so that the specimen length to width aspect ratio was 20 to 1 (insuring true uniaxial stress states).

All uniaxial stress-strain and creep tests in this paper were conducted at room temperature (25 °C). The strain rate for the stress-strain testing was $\dot{\varepsilon}$ = 0.001 sec^{-1}, while the applied stress for the creep testing was σ = 15 MPa.

Typical Tensile and Creep Test Data

A typical recorded tensile stress strain curve for solder with labeled standard material properties is shown in Figure 9. The notation "E" is taken to be the effective elastic modulus, which is the initial slope of the stress-strain curve. Since solder is viscoplastic, this effective modulus will be rate dependent, and will approach the true elastic modulus as the testing strain rate approaches infinity. The yield stress σ_Y (YS) is taken to be the standard .2% yield stress (upon unloading, the permanent strain is equal to $\varepsilon = .002$). Finally, the ultimate tensile strength σ_u (UTS) is taken to be the maximum stress realized in the stress-strain data. As shown in Figure 9, the solders tested in this work illustrated nearly perfect elastic-plastic behavior (with the exception of a small transition region connecting the elastic and plastic regions). As the strain level becomes extremely high and failure is imminent, extensive localized necking takes place. These visible reductions in cross-sectional area lead to non-uniform stress-states in the specimen and drops in the applied loading near the end of the stress-strain curve.

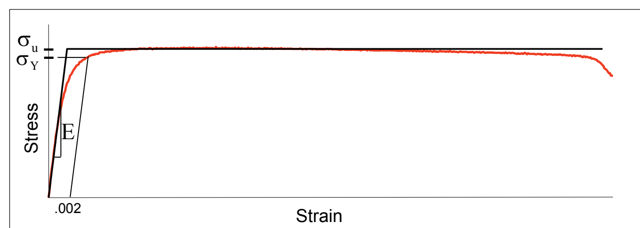

Figure 9 - Typical Solder Stress-Strain Curve and Material Properties

For the uniaxial stress-strain tests, a total of 10 specimens have been tested for each mixed solder alloy at each set of aging conditions. From the recorded stress-strain data, a set of averaged material properties were extracted. Variations of the average mechanical properties (elastic modulus, yield stress, ultimate strength, creep compliance, etc.) with aging were observed and then modeled as a function of aging time. In our prior work [23], we have demonstrated that it is possible to replace a set of 10 recorded stress-strain curves for a certain testing configuration with a single "average" curve that accurately represents the observed response for all strain levels. Although, several different mathematical models can be used to represent the observed data, we have chosen to use a linear model for extremely small strains ($\varepsilon << .001$), and a four parameter empirical representation called the Weibull model for larger strains:

$$\begin{aligned} \sigma(\varepsilon) &= E\varepsilon & \varepsilon \le \varepsilon^* \\ \sigma(\varepsilon) &= A_0 - A_1 e^{-A_2 \varepsilon^{A_3}} & \varepsilon \ge \varepsilon^* \end{aligned} \tag{2}$$

where E is the initial elastic modulus; A_0, A_1, A_2, A_3 are material constants to be determined; and ε^* is the strain level where the two functions cross (become equal). The two function approach is typical for elastic-plastic materials, where it is desirable to model the initial portion of the stress-strain curve as perfectly linear (elastic), and the remaining portion of the curve as nonlinear.

Figure 10 illustrates a typical set of 10 solder stress strain curves measured under similar conditions, and the corresponding fit of eq. 2 to the data. The excellent representation provided by the elastic-plastic empirical model suggests that it indeed provides a mathematical description of a suitable "average" stress-strain curve for a set of experimental curves measured under fixed test conditions.

Figure 11 illustrates a typical solder creep curve (strain vs. time response for a constant applied stress). The response begins with a quick transition to the initial "elastic" strain level, followed by regions of primary, secondary, and tertiary creep. Depending on the applied stress level, the primary creep region can be more extensive for the SAC alloys

relative to Sn-Pb solders. The secondary creep region is typically characterized by a very long duration of nearly constant slope. This slope is referred to as the "steady state" secondary creep rate or creep compliance, and it is often used by practicing engineers as one of the key material parameters for solder in finite element simulations used to predict solder joint reliability. In this work, the measured creep rates were taken to be the minimum slope values in the secondary creep regions of the observed $\dot{\varepsilon}$ versus t responses. The tertiary creep region occurs when rupture is imminent, and typically features an abrupt change to a nearly constant but significantly increased creep rate.

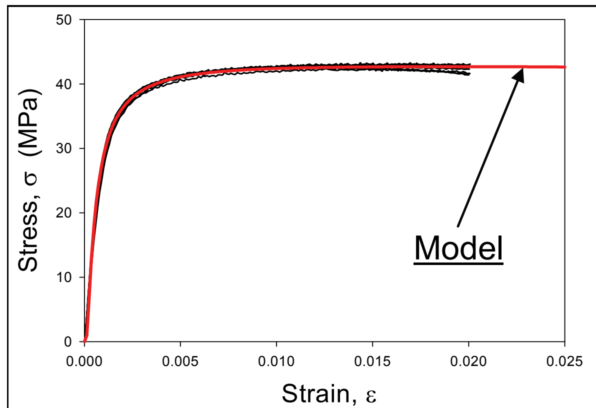

Figure 10 - Solder Stress-Strain Curves and Empirical Model

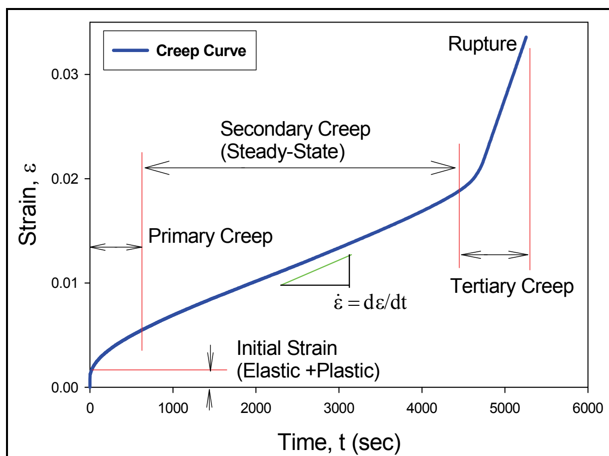

Figure 11 - Typical Solder Creep Curve

In the solder creep experiments, constant stress levels on the order of 25-50% of the observed UTS were applied. For the data presented in this paper, the applied stress was σ = 15 MPa, which is approximately 25%-33% of the non-aged UTS values for the various alloys tested. Due to the long test times involved, only 5 specimens were tested for each alloy for any given set of aging conditions. From the recorded strain vs time curves under constant stress, the "steady state" creep strain rates have been extracted. In practice, the measured creep rate for each curve was evaluated numerically by calculating the minimum slope value in the secondary creep region of the observed $\dot{\varepsilon}$ versus t response.

Results and Analysis

Physical properties

The variations of solidification properties such as melting temperature and pasty range for the solders of different mixture ratios have been evaluated by DSC analysis. Results are plotted in Figures 12-13, with the horizontal axes in each graph indicating the wt% of Sn-Pb (0% = SAC305 is on the left, and 100% = Sn-Pb is on the right). As the level of Sn-Pb in the mixture is increased, it is observed that the melting temperature of mixed solders decreases as expected until 30% of the alloy is Sn-Pb. At that point, the melting temperature is approximately constant (at or slightly below the Sn-Pb level of 183 ^{o}C). It also can be seen that the pasty range of mixed formulation solders becomes large as the mixture nears the two extreme compositions of pure SAC or pure Sn-Pb. For mixtures between 30-70% Sn-Pb, the pasty range is very small (less than 2 ^{o}C).

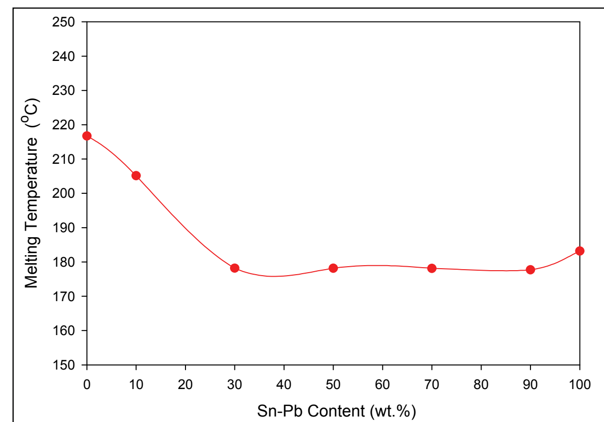

Figure 12 - Melting Temperature vs. Sn-Pb Content

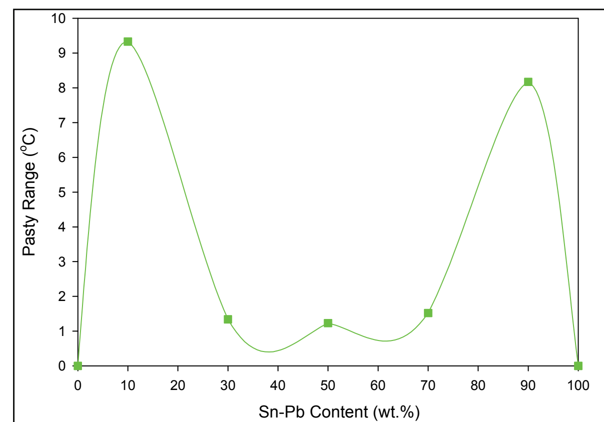

Figure 13 - Pasty Range vs. Sn-Pb Content

Microstructural Evolution

The microstructural changes occurring with different mixture ratios have been evaluated by Scanning Electronic Microscopy. Figure 14 contains micrographs of the seven mixed formulations solders recorded at 3500X. The well-known microstructure of pure SAC305, i.e. bundles of needle-shaped Ag_3Sn particles distributed on Sn matrix can be found in the first picture of the series. However, as the content of Sn-Pb increases in the mixtures, the Ag_3Sn particles change dramatically into thin and bone-shaped precipitates distributed across the Sn matrix. EDX analysis shows that these precipitates are rich in Ag and Pb. As the Sn-Pb content increases from 10% to 90%, the precipitates in the mixed formulation solders evolve from thin bone-shaped to thick bone-shaped to coarse bone-shaped to pie-shaped, and finally, to coarse pie-shaped particles. Eventually, as the Sn-Pb content reaches 100%, the typical eutectic structure is observed (last picture of the series). Since mechanical properties are ultimately determined by microstructure, the distinctive microstructures of mixed formulation solder alloys will have determinative effects on their mechanical performance.

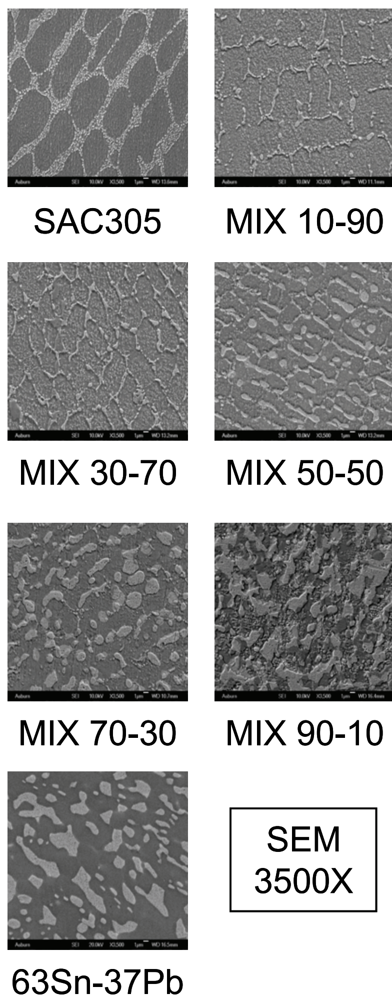

Figure 14 - Microstructure of Mixed Solders

Stress-Strain Tensile Testing

As discussed above, the uniaxial test specimens were solidified in glass tubes. A rapid cooling profile (water quenching) was utilized to yield fine microstructures and to illustrate the upper limit of mechanical properties and the lower limit of possible creep rates for the various mixed alloys. The samples were isothermally aged for various durations in the range 0-60 days at 25 ^{o}C (room temperature) as well as 100 ^{o}C (elevated temperature). For each set of aging conditions (aging temperature, aging time), 10 specimens were tested at room temperature (T = 25 °C) and an average stress-strain curve was found by fitting eq. (2) to the measured data. Figures 15-21 illustrate the stress-strain results (fitted curves) for the seven alloys.

The material properties (stiffness and strength) were extracted from the stress-strain data. Figures 22-24 illustrate the variations of elastic modulus, yield strength, and ultimate tensile strength (UTS), respectively, for the original (non-aged) samples with the Sn-Pb content of the mixed formulation solder. It is observed that the highest material properties are found for the SAC305 material with no Sn-Pb. As the level of Sn-Pb is increased, the elastic modulus and yield strength decline slowly in a linear manner from 0 to 90% Sn-Pb content. A sudden drop then occurs, as the mixture becomes pure (100%) Sn-Pb. The behavior of the UTS is more complicated/nonlinear. However, the UTS can be visualized as approximately constant from 0-90% Sn-Pb, with a rapid decline as the level of Sn-Pb approaches 100%.

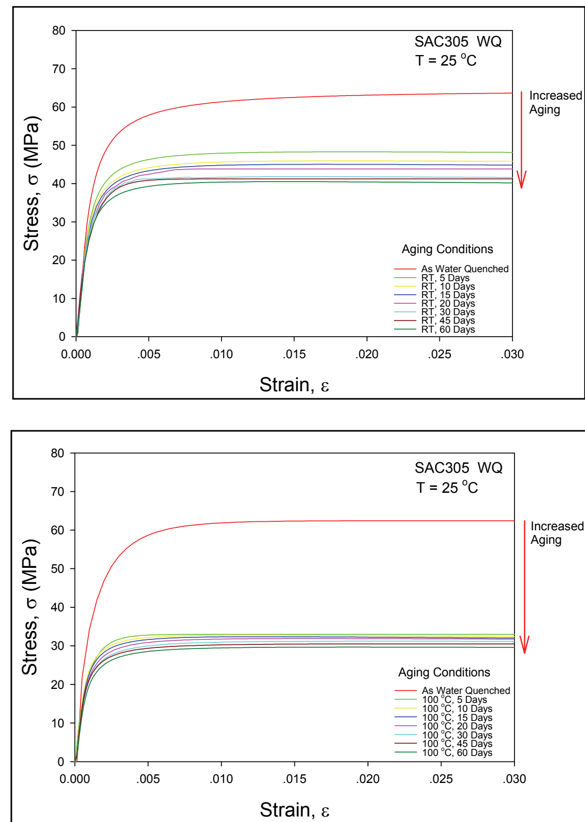

Figure 15 - Stress-Strain Curves for MIXED 0-100 (SAC305)

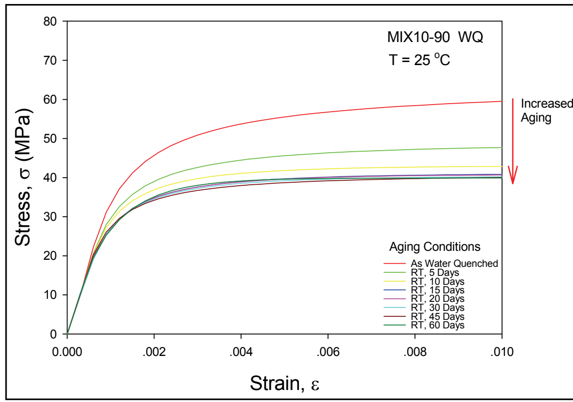

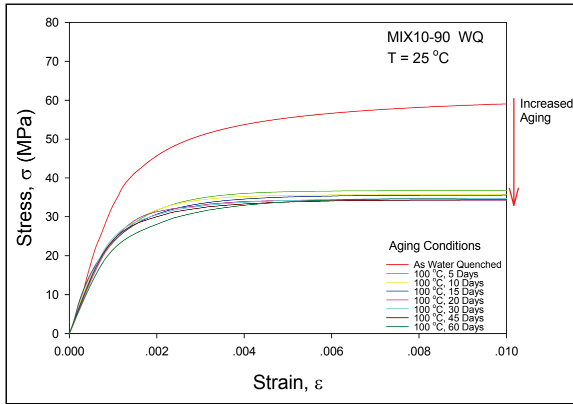

Figure 16 - Stress-Strain Curves for MIXED 10-90

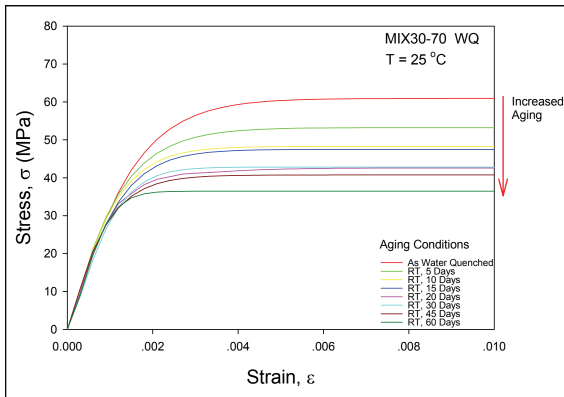

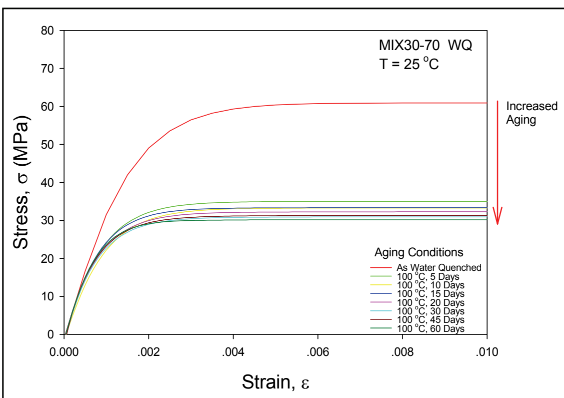

Figure 17 - Stress-Strain Curves for MIXED 30-70

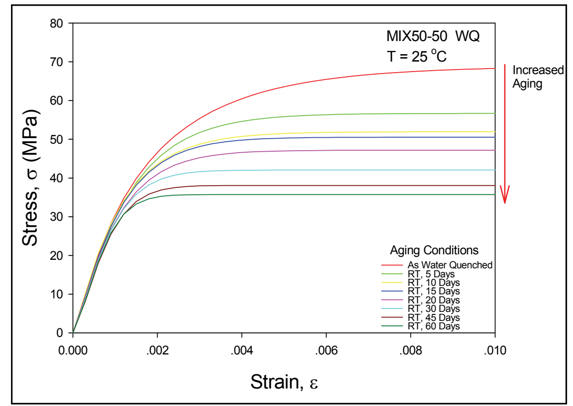

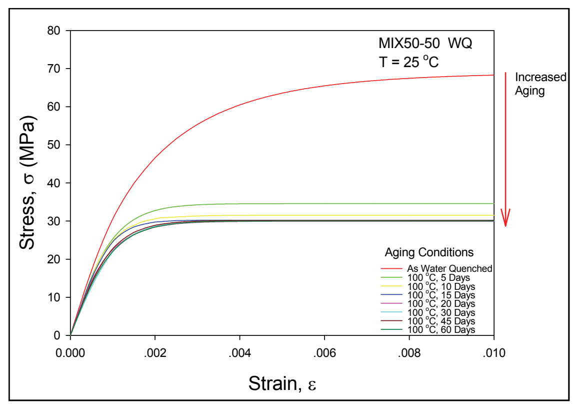

Figure 18 - Stress-Strain Curves for MIXED 50-50

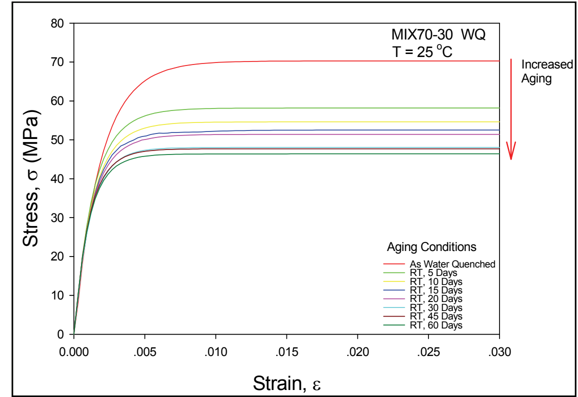

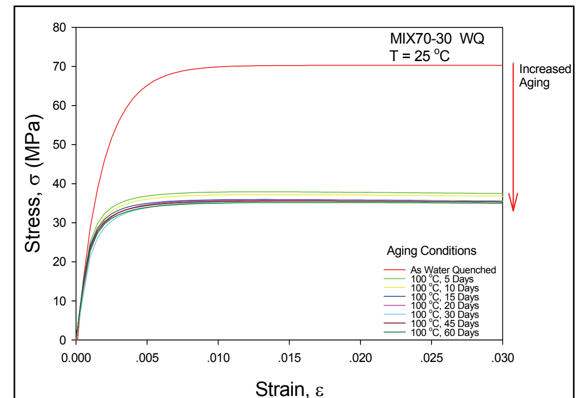

Figure 19 - Stress-Strain Curves for MIXED 70-30

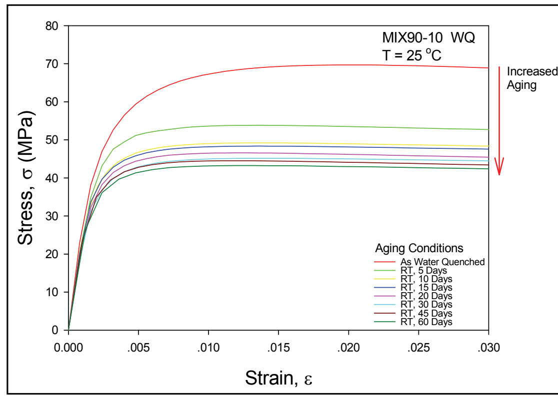

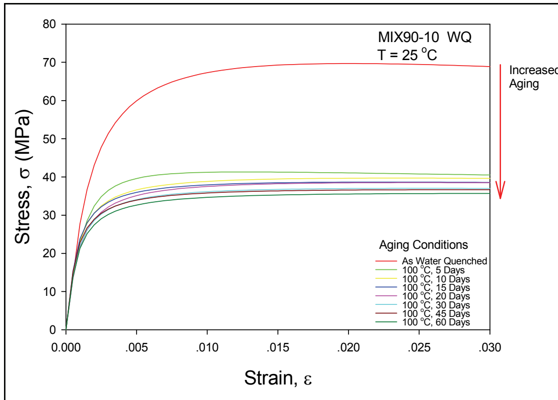

Figure 20 - Stress-Strain Curves for MIXED 90-10

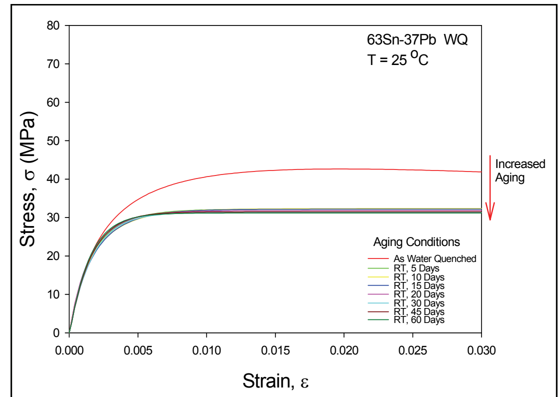

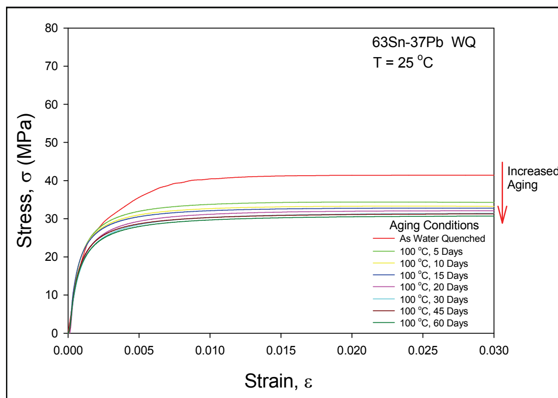

Figure 21 - Stress-Strain Curves for MIXED 100-0 (Sn-Pb)

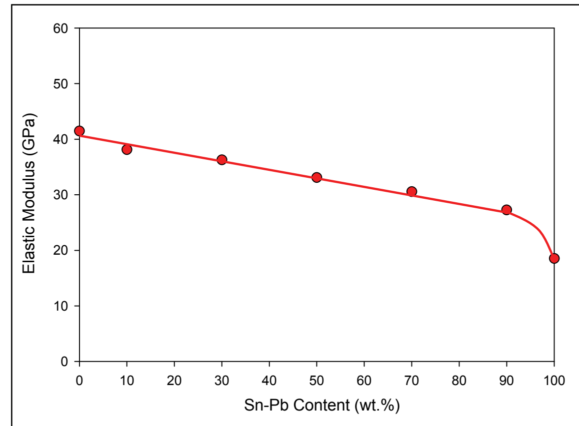

Figure 22 - Variation of Elastic Modulus with Sn-Pb Content [No Aging]

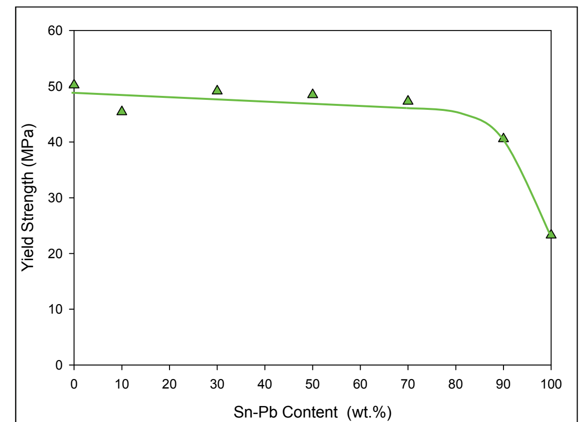

Figure 23 - Variation of Yield Strength with Sn-Pb Content [No Aging]

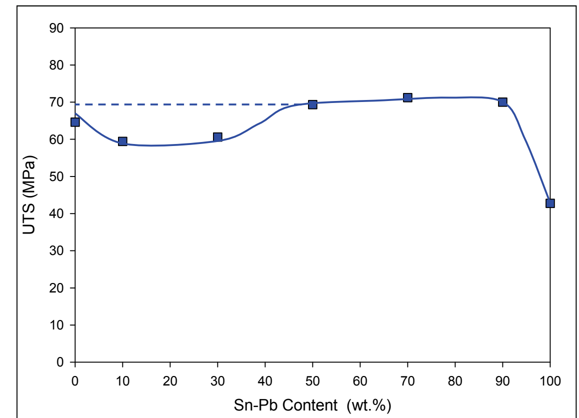

Figure 24 - Variation of UTS with Sn-Pb Content [No Aging]

As shown in our prior study [23] on aging of SAC and Sn-Pb alloys, the material properties of solders evolve with aging. The variations of the properties of the seven mixed formulation solders with aging time are shown in Figures 25-

27, for the elastic modulus, yield strength, and ultimate tensile strength (UTS), respectively.

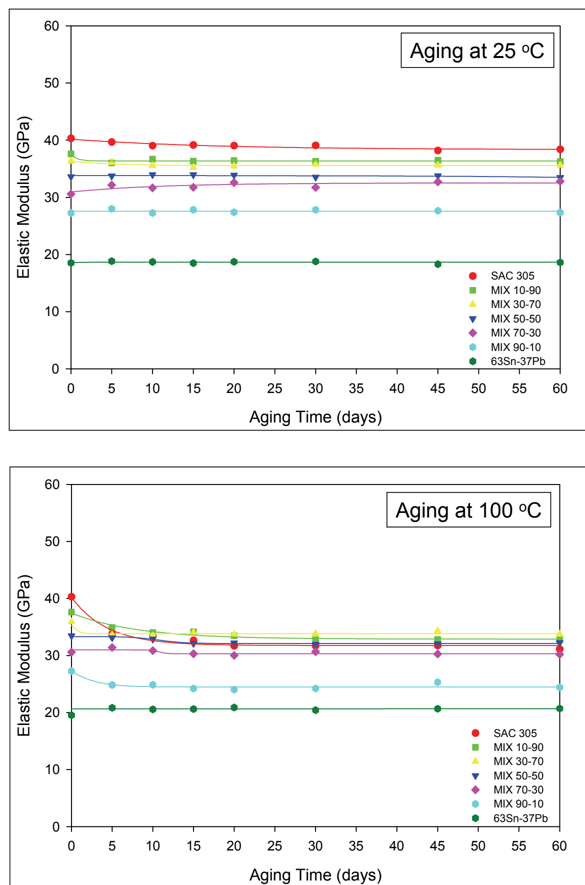

Figure 25 - Variation of the Elastic Modulus with Aging

From the graphs in Figure 25, it is observed that the effective elastic modulus remains almost constant for all of the mixed alloys over the 60-day period of aging. The largest changes are observed for pure SAC305 that is aged at 100 ^{o}C. Thus, having some amount of Pb in your solder joint is good from the point of view of blunting the effects of aging on the solder stiffness. As seen in Figures 26-27, the effects of aging on the yield strength and ultimate strength of the solders are much more dramatic. The majority of the changes occur during the first 15 days for aging at 25 ^{o}C, and in the first 5 days for aging at 100 ^{o}C. The largest relative changes are again seen for the pure SAC305 alloy (no Pb), while the smallest relative changes are seen for the pure Sn-Pb alloys (most Pb). Thus, Pb is again seen to aid in the resistance to aging induced strength degradations. With large aging times, the strengths of the mixed alloys appear to be approaching nearly constant values. More careful analysis has revealed that the SAC305 alloy and the mixed alloys closest to SAC305 (e.g. MIX 10-90) are still degrading in a slow linear manner with aging time. This phenomenon has been explored in detail in reference [23].

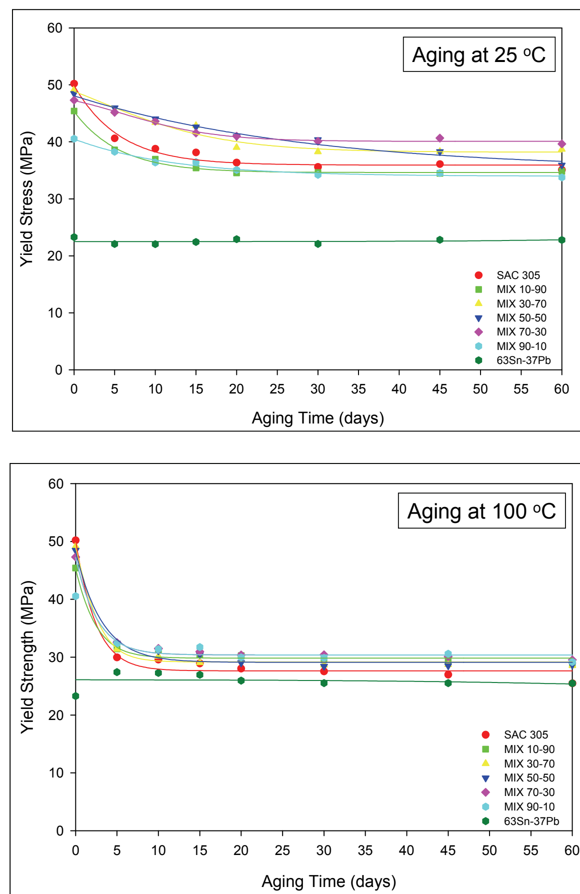

Figure 26 - Variation of the Yield Strength with Aging

The distinctive microstructures of the mixed formulation solders can be used to explain some aspects of the mechanical property variations. For example, the needle shaped precipitates in SAC 305 play a dual role, i.e. they strengthen the material as hard particles but at the same time, they lead to material failure by providing a source and path for crack initiation and propagation. Similarly, the precipitates in the MIX 50-50 solder also are potential sources of cracks rather than a material strengthener, due to their bone-like shape and softer nature when compared to the Ag_3Sn particles in SAC305. It is known that this kind of precipitate is detrimental to mechanical properties. However, as the Sn-Pb content exceeds 50%, coarsening processes takes place and the precipitates change from bone-shaped particles into pie-shaped particles. Even though these particles are not as strong as those in SAC 305, their unique morphology hinders the formation of cracks, and retards the spread of cracks across the matrix. Therefore, they help improve the mechanical properties of the mixed solders.

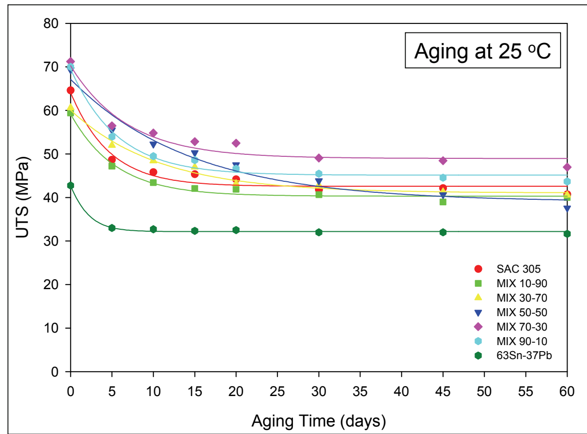

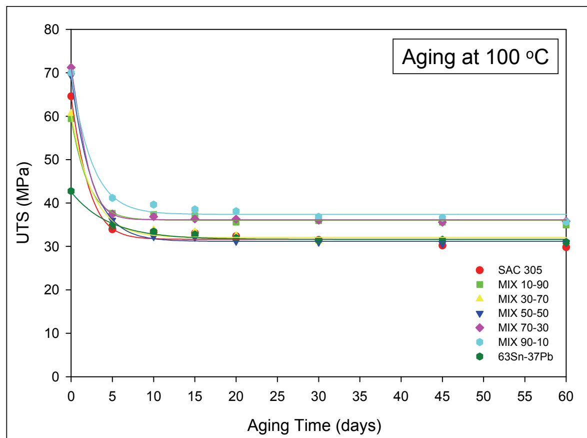

Figure 27 - Variation of the UTS with Aging

Creep Testing

The uniaxial specimens for the various mixed solder alloys were aged at 25 °C (room temperature) and 100 °C (elevated temperature) for up to 60 days. After aging, a constant stress level of 15 MPa was applied to the samples at T = 25 °C. The stress level is about 20-25% of the UTS values of the as quenched solder samples. Specimen groups of five were prepared for each alloy and set of aging conditions. Figures 28-29 illustrate the typical recorded creep curves for the MIX 50-50 solder alloy for aging at 25 °C and 100 °C, respectively. In each graph, the various creep curves are for different aging times, illustrating the evolution of the creep response with duration of aging. For brevity and clarity of the presentation, only one of the five available creep curves is shown in each plot for each set of aging conditions. Similar results were obtained for the other six mixed solder alloys. A plot of the variation of the secondary creep rate with Sn-Pb content (no aging) is shown in Figure 30. It is observed that the creep rates for the as cast samples are nearly constant for up to 70% Sn-Pb content.

The plots in Figure 29 clearly indicate a dramatic evolution of the creep response of the mixed alloy with aging at elevated temperature (100 °C). The effect is less pronounced (but present) for room temperature aging. The effects of aging on the creep rate can be better seen by plotting the extracted secondary creep rates versus the aging time for each alloy. Such graphs are presented for all seven mixed alloys in Figures 31 and 32 for aging at 25 °C and 100 °C, respectively. Each data point represents the average creep rate measured for the 5 samples tested at a given set of aging conditions. For each alloy and aging temperature, the data points were fit well with a log-exponential relationship:

$$\log \dot{\varepsilon} = C_0 + C_1 t + C_2 (1 - e^{-C_3 t}) \tag{3}$$

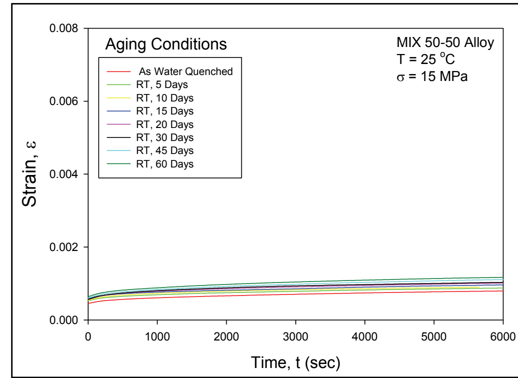

Figure 28 - Creep Curves for MIX 50-50 Alloy [Aging at 25 °C]

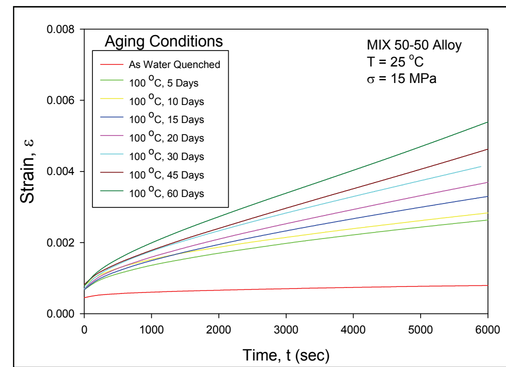

Figure 29 - Creep Curves for MIX 50-50 Alloy [Aging at 100 °C]

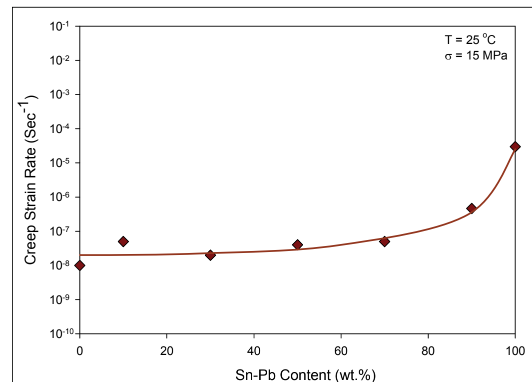

Figure 30 - Variation of Creep Rate Sn-Pb Content [No Aging]

If the strain rate versus aging time data is plotted with a log scale on the vertical axis (as in Figures 31-32), constant C_0 is the intercept and constant C_1 is the slope of the linear part of the curve for large aging times. Constants C_2 and C_3 are associated with the nonlinear transition region in the first 10-30 days of aging. The creep rate for Sn-Pb is relatively stable with aging, even at elevated temperature. As aging progresses, the creep rates of SAC305 and many of the other mixed alloys will continue to increase with time and eventually "cross-over" or exceed the creep rate of Sn-Pb [23].

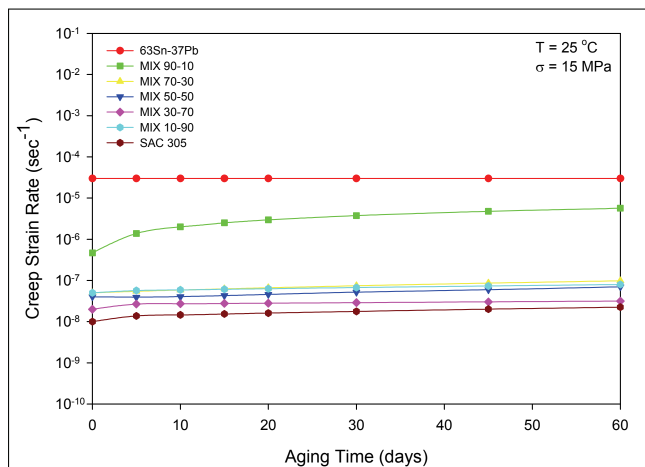

Figure 31 - Variation of the Creep Rate with Aging at 25 °C

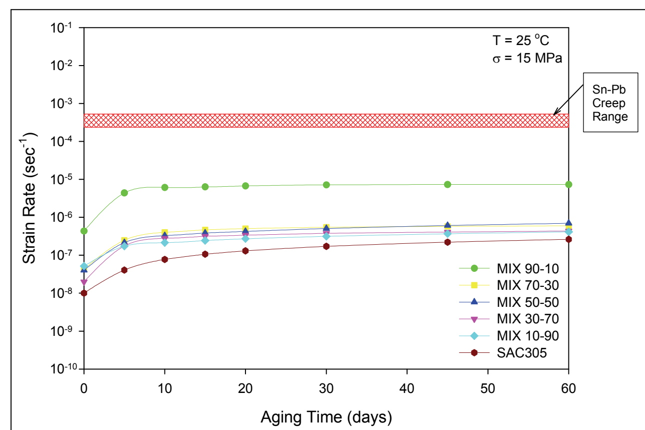

Figure 32 - Variation of the Creep Rate with Aging at 100 °C

Summary and Conclusions

In this work, we have explored the physical properties and mechanical behavior of mixed formulation solder materials. Seven different mixture ratios of 63Sn-37Pb and SAC305 solder materials have been formed, which include five carefully controlled mixtures of the two solder alloys (by weight percentage) and the two extreme cases (pure Sn-Pb and pure SAC). For the various percentage mixtures, the melting point, pasty range, stress-strain curves, mechanical properties (modulus, strength, elongation), and creep curves have been characterized.

The melting point of the mixed solders decreased as expected until 30% of the alloy was Sn-Pb. At that point, the melting temperature was approximately constant (at or slightly below the Sn-Pb level of 183 °C). It was also observed that the pasty range of the mixed solders became large as the mixture neared the two extreme compositions of pure SAC or pure Sn-Pb. For mixtures between 30-70% Sn-Pb, the pasty range was very small (less than 2 °C). The microstructures realized with the various mixtures were found, and the various shapes and compositions of the intermetallic phases were identified and correlated to the mechanical measurements.

The variations of the mechanical properties and creep rates with aging at room temperature (25 C) and elevated temperature (100 C) have also been measured. It was observed that the effective elastic modulus remains almost constant for all of the mixed alloys over the 60-day period of aging. The largest changes were observed for pure SAC305 that is aged at 100 °C. Thus, having some amount of Pb in your solder joint is good from the point of view of blunting the effects of aging on the solder stiffness. The effects of aging on the yield strength and ultimate strength of the solders were much more dramatic. The majority of the changes occurred during the first 15 days for aging at 25 °C, and in the first 5 days for aging at 100 °C. The largest relative changes were again seen for the pure SAC305 alloy (no Pb), while the smallest relative changes were seen for the pure Sn-Pb alloy (most Pb). Thus, Pb is again seen to aid in the resistance to aging induced strength degradations. The creep response of the mixed alloys dramatically evolved with aging, with pure Sn-Pb having the smallest changes.

Acknowledgments

This work was supported by Basic Research Grant # IIP-0434909-015 from the National Science Foundation, as well as the NSF Center for Advanced Vehicle Electronics (CAVE).

References

1. Nandagopal, B., Mei, Z., and Teng, S., "Microstructure and Thermal Fatigue Life of BGAs with Eutectic Sn-Ag-Cu Balls Assembled at 210 C with Eutectic Sn-Pb Solder Paste," *Proceeding of the 56th Electronic Components and Technology Conference*, pp. 875-883, 2006.
2. Evans, J. L., Mitchell, C., Bozack, M., and Payton, L. N., "Reliability of SAC BGA Using SnPb Paste for Harsh Environment Electronics," *Proceedings of the SMTA International Conference*, 2005
3. Handwerker, C., "Transitioning to Lead-Free Assemblies," *Printed Circuit Design and Manufacture*, pp. 17-23, 2005.
4. Hua, F., Aspandiar, R., Clemons, G., and Chung, C. K., "Solder Joint Reliability Assessment of Sn-Ag-Cu BGA Components Attached with Eutectic Pb-Sn Solder," *Proceedings of the SMTA International Conference*, pp. 246-252, 2005.

5. Kannabiran, A., Elavarasan, T., Pannerselvam, and S., Ramkumar, M., “Investigation of the Forward And Backward Compatibility of Solder Alloys with Component Finishes For HASL and OSP PCB Finish,” *Proceedings of the SMTA International Conference*, pp. 566-570, 2006.
6. Heather McCormick, H., Snugovsky, P., Bagheri, Z., “Mixing Metallurgy: Reliability of SAC Balled Area Array Packages Assembled Using SnPb Solder”, *Proceedings of the SMTA International Conference*, pp. 425-432, 2006.
7. Abtew, M., and Kinyanjui, R., “Effect of Inert Atmosphere Reflow and Solder Paste Volume on the Microstructure and Mechanical Strength of Mixed Sn-Ag-Cu and Sn-Pb Solder Joints,” *Proceedings of the SMTA International Conference*, pp. 74-78, 2006.
8. Chatterji, I., “Backward Compatibility, Are We Ready - A Case Study”, *Proceedings of the SMTA International Conference*, pp. 416-424, 2006.
9. Zbrzezny, A. R., Snugovsky, P., Lindsay, T., and Lau, R., “Reliability Investigation of Mixed BGA Assemblies,” *IEEE Transactions on Electronics Packaging Manufacturing*, Vol. 29(3), pp. 211-216, 2006
10. Hillman, D., Wells, M., Cho, K., and Collins, R., “The Impact of Reflowing a Pbfree Solder Alloy Using a Tin/Lead Solder Alloy Reflow Profile on Solder Joint Integrity,” *Proceedings of the Lead-Free Conference*, CMAP Toronto, pp. 1-9, 2005.
11. Hua, F., Aspandiar, R., Rothman, T., and Anderson, C., “Solder Joint Reliability of Sn-Ag-Cu BGA Components Attached with Eutectic Pb-Sn Solder Paste,” *Proceedings of the SMTA International Conference*, 2001.
12. Theuss, H., Kilger, T., and Ort, T., “Solder Joint Reliability of Lead-free Solder Balls Assembled with SnPb Paste,” *Proceeding of the 53rd Electronic Components and Technology Conference*, pp. 331-337, 2003.
13. Nandagopal, B., “Study on Assembly, Rework Process, Microstructures and Mechanical Strength of Backward Compatible Assembly,” *Proceedings of the SMTA International Conference*, pp. 861-870, 2005.
14. Nguyen, J., and Shangguan, D., “Solder Joint Characteristics and Reliability of Lead-Free Area Packages Assembled Under Various Tin-Lead Soldering Process Conditions,” *Proceeding of 57th Electronic Components and Technology Conference*, pp. 1340-1349, 2007.
15. Sun, F., “Solder Joint Reliability of Sn-Ag-Cu BGA and Sn-Pb Solder Paste,” *Proceeding of 6th International Conference on Electronic Packaging Technology*, 2006.
16. Chung, C. K., Aspandiar, R., Leong, K. F., Tay, C. S., “The Interactions of Lead (Pb) in Lead Free Solder (Sn/Ag/Cu) System,” *Proceeding of 52nd Electronic Components and Technology Conference*, pp. 168-175, 2002.
17. Hunt, C., Nottay, J., Brewin, A., and Dinsdale, A., “Predicting Microstructure of Mixed Solder Alloy System”, *NPL Report*, MATC(A) 83, April 2002.
18. Bath, J., Hu, L., and Chiang, D., “Reliability Evaluation Of Lead-Free SnAgCu PBGA676 Components Using Tin-Lead and Lead-Free SnAgCu Solder Paste,” *Proceedings of the SMTA International Conference*, pp. 891-901, 2005.
19. Clech, J. P., “Lead-Free and Mixed Assembly Solder Joint Reliability Trends,” *Proceedings of APEX 2004*, Paper S28-3, pp. 1-14, 2004.
20. Nguyen, J., Geiger, D., Rooney, D., and Shangguan, D., “Reliability Study of Lead-Free Area Array Packages with Tin-Lead Soldering Processes”, *Proceedings of the SMTA International Conference*, pp. 433-438, 2006.
21. Choubey, A., and Menschow, D., “Effect of Aging on Pull Strength of SnPb, SnAgCu, and Mixed Solder Joints in Peripheral Surface Mount Components,” *Journal of SMTA*, Vol. 19(2), pp. 33-37, 2006.
22. Jiang, T. B., Du, C., and Xu L. H., "Finite Element Analysis and Fatigue Life Prediction of BGA Mixed Solder Joints,” *Proceedings of High Density Packaging and Microsystem Integration - HDP '07*, pp. 1-6, 2007.
23. Ma, H., Suhling, J. C., Zhang, Y., Lall, P., and Bozack, M. J., “The Influence of Elevated Temperature Aging on Reliability of Lead Free Solder Joints,” *Proceedings of the 57th IEEE Electronic Components and Technology Conference*, pp. 653-668, Reno, NV, May 29-June 1, 2007.